SPIN-LADDER IRON OXIDE: $Sr_3Fe_2O_5$

H. Kageyama[1], T. Watanabe[1], Y. Tsujimoto[1], A. Kitada[1], Y. Sumida[1], K. Kanamori[1], K. Yoshimura[1], N. Hayashi[2], S. Muranaka[2], M. Takano[3, 4], M. Ceretti[5], W. Paulus[5], C. Ritter[6], G. André[7]

[1]Department of Chemistry, Graduate School of Science, Kyoto University, Japan
[2]Graduate School of Human and Environmental Studies, Kyoto University, Japan
[3] Institute for Chemical Research, Kyoto University, Uji, Japan
[4] Institute for Integrated Cell-Materials Sciences and Research Institute for Production Development, Japan
[5] University of Rennes1, Sciences Chimiques de Rennes UMR CNRS 6226, Campus de Beaulieu, Rennes
[6] Institute Laue Langevin, BP 156, 38042, Grenoble, France
[7] Laboratoire Léon Brillouin, CEA-CNRS Saclay, 91191, Gif-sur-Yvette, France

The concept of "spin ladder" originally appeared to study the theoretically still controversial antiferromagnet (AF) 2D square lattice in high-temperature superconducting cuprates starting from a well understood 1D AF chain [1-2]. They can been schematized as an array of finite number of coupled chains .The motivation of theoretical investigations has been to test how the one-dimensional (1D) S=1/2 AF chain system (n=1), that is rigorously solved even when doped with carriers, could be connected to the 2D square lattice (n=∞) that in turn encounters various theoretical difficulties and is far from being understood. Experimentally, $Sr_{n-1}Cu_nO_{2n-1}$ has been the only example representing a generalized spin-ladder system [3-5].

The utmost structural characteristic of cupric (Cu^{2+}; d^9) oxides is the favored formation of the square-planar CuO_4 units, which are stabilized due to the Jahn-Teller effect [6]. This 2D coordination geometry provides strong exchange interactions within a ladder along the leg and the rung, while the interaction normal to the square plane is negligibly small due to the lack of superexchange pathways involving oxide ions. Unlike in the case of cuprates, the coordination geometries in iron oxides have been almost exclusively restricted to 3D polyhedra such as octahedra and tetrahedra. However, this barrier has recently been overcome [7], using electropositive calcium hydride at low temperatures as a reductant, the low-temperature reaction of a cubic perovskite $SrFe^{4+}O_3$ with CaH_2 stabilized $SrFe^{2+}O_2$ with a square-planar oxygen coordination around the high-spin Fe^{2+} ion. The structure is isostructural with the "infinite" layer cupric oxides.

For the first time we show the synthesis of a novel spin-ladder iron oxide $Sr_3Fe^{2+}_2O_5$ through the reaction of the double-layered perovskite $Sr_3Fe^{4+}_2O_7$ with CaH_2 [8]. By using neutron diffraction, synchrotron X ray diffraction and Mössbauer, we provide a complete characterization of this first spin ladder iron oxide.

A slightly oxygen deficient phase $Sr_3Fe_2O_{7-y}$ (y~0.4) could be easily prepared by a conventional, high-temperature solid-state reaction and was used as a precursor. For $Sr_3Fe_2O_{7-y}$ all oxygen vacancies are located at the apical O(1) sites shared by the double FeO_2 sheets (Figure 1 a and b)and the structure keeps the $I4/mmm$ space group over the entire range from $Sr_3Fe_2O_7$ (y=0) to $Sr_3Fe_2O_6$ (y=1) [9].
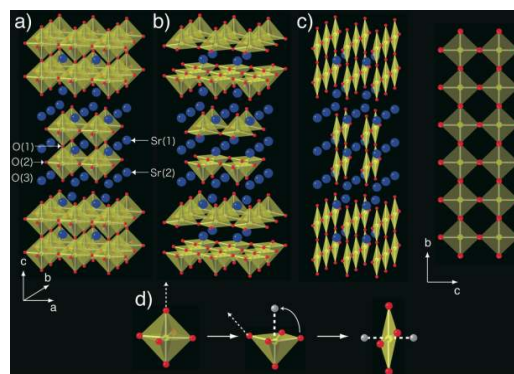
Fig. 1. Structural transformation from $Sr_3Fe_2O_7$ to $Sr_3Fe_2O_5$ via $Sr_3Fe_2O_6$, where the blue, red, and yellow spheres represent Sr, O, and Fe atoms, respectively. a) Crystal structure of a stoichiometric (fully oxidized) phase $Sr_3Fe_2O_7$ (y=0). b) Crystal structure of reduced phase $Sr_3Fe_2O_6$ (y=1), once thought to be the lower limit of the oxygen content. c) Left: Crystal structure of the new phase $Sr_3Fe_2O_5$ (y=2), described herein. Right: A spin ladder in $Sr_3Fe_2O_5$ viewed along the a axis. d) Transformation from the octahedron (left) in $Sr_3Fe_2O_7$ to the pyramid (middle) in $Sr_3Fe_2O_6$ and to the square plane (right) in $Sr_3Fe_2O_5$, where the white spheres represent oxygen vacancies.

The powder X-ray diffraction (XRD) pattern of the present precursor also indicated a tetragonal $I4/mmm$ cell with a = 3.872 Å and c = 20.157 Å. To prepare $Sr_3Fe_2O_5$, $Sr_3Fe_2O_{6.6}$ (0.43 g) and a two-molar excess of CaH_2 were finely ground and pelletized in an argon-filled drybox, sealed in an evacuated glass tube, and brought to reaction at 623 K for 3 days. The final product was washed to remove undesirable residues, CaH_2 and CaO, with a dried 0.1 M NH_4Cl/methanol solution. The Fe-oxide thus obtained is quite air-sensitive so that all the chemical and physical characterizations were conducted with efforts to minimize exposure to air. Synchrotron powder XRD pattern of the final product taken at the SPring-8 (Japan) BL02B2 beam line (λ= 0.777 Å) showed that $Sr_3Fe_2O_5$ adopts the $Immm$ space group (No. 71), with a = 3.51685(5) Å, b = 3.95405(7) Å, c = 20.91727(36) Å. Neutron powder diffraction (DIA at ILL and G4.1 at the LLB) analysis at 293 K confirmed the above structure and it also excluded a possibility that hydrogen atoms are incorporated into the lattice. Furthermore, Mössbauer measurements (Figure 2a) indicated not only that all the Fe atoms are electronically and

crystallographically equivalent, but also that they are most likely square-planar coordinated in high-spin state (S=2), since the obtained isomer shift (IS) of 0.46 mms^{-1}, quadrupole splitting ΔE of 1.28 mms^{-1} at 300 K, and the magnetic hyperfine field of H_{hf}=43.7 T at 4 K are close to those of $SrFeO_2$ [9]. These observations are consistent with the structural analysis. Neutron powder diffraction data down to 1.4 K on G41 (LLB, λ=2.42 Å) (Figure 2b) and D1A (ILL, λ=1.91 Å) revealed that the long-range AF order is characterized by a magnetic propagation vector q= (1/2, 1/2, 0) and that the iron moments of 2.76(5) μ_B are aligned parallel to the c axis.

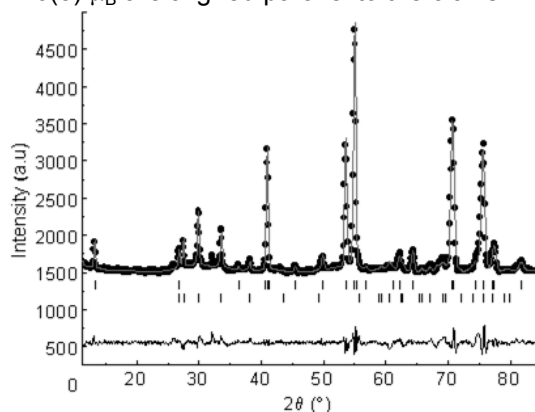*Fig 2b) Rietveld refinement of NPD data at 1.4 K measured at 2.42 Å on G4.1 (LLB). The solid lines and the overlying crosses and bars indicate the calculated intensities, the observed intensities, and the positions of the calculated nuclear (top) and magnetic (bottom) Bragg reflections. The difference between the observed and calculated profiles is plotted at the bottom.*

It is noteworthy that there are neither intermediate phases nor nonstoichiometry between $Sr_3Fe_2O_6$ and $Sr_3Fe_2O_5$, as well as between $SrFeO_{2.5}$ and $SrFeO_2$. This is remarkable given the presence of two intermediates, $SrFeO_{2.875}$ and $SrFeO_{2.75}$, between $SrFeO_3$ and $SrFeO_{2.5}$. It is also known that electrochemical formation of $SrCoO_3$ from $SrCoO_{2.5}$, which are isomorphous with $SrFeO_3$ and $SrFeO_{2.5}$, respectively, proceeds topotactically at room-temperature via the complex vacancy-ordered intermediate phase $SrCoO_{2.82\pm\_0.07}$[10]. The processes occurring in the formation of $SrFeO_2$ from $SrFeO_{2.5}$, whereby the FeO_4 tetrahedra and the FeO_6 octahedra linked to each other are both converted to FeO_4 squares [11] must be more complicated than the case discussed above. We now recognize that the underlying perovskite and related lattices are flexible enough to tolerate such drastic compositional and structural events. We thus believe that oxygen transport materials working at low temperatures that feature formation of intermediate ordered structures should be promising.

Finally, we must assume that the present synthetic strategy involving CaH_2 reduction can be further generalized for a more rational design of new magnetic lattices comprising extended arrays of FeO_4 square planes, for which formerly only copper(II) oxides were candidates.
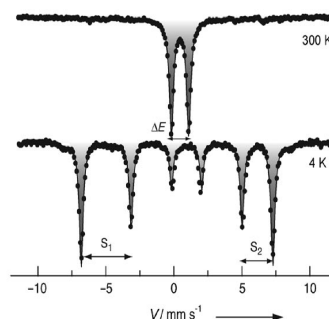
(b)

Fig. 2a). Magnetic order in $Sr_3Fe_2O_5$. a) Mössbauer spectra at 300 (top) and 4 K (bottom). The circles indicate the experimental data, while the lines denote the fits.

References :

[1] Dagotto, E., Rice, T. M. *Science* **271**, 618-623 (1996)
[2] Dagotto, E.. *Rep. Prog. Phys.* **62**, 1525-1571 (1999)
[3] Azuma, M. Hiroi, Z. Takano, M. Ishida, K., Kitaoka, *Phys. Rev. Lett.* **73**, 3463-3466 (1994)
[4] Kojima, K. *et al*.. *Phys. Rev. Lett*. **74**, 2812-2815
[5] Hiroi, Z. Azuma, M. Takano, M. & Bando, Y. *J. Solid State Chem.* **95**, 230-238 (1991)
[6] Azuma, M. Fujishiro, Y. Takano, M. Nohara, M. & Takagi, H. *Phys. Rev. B* **55**, R8658-R8861 (1997).
[7] Tsujimoto, C. Tassel, N. Hayashi, T.Watanabe, H. Kageyama, K. Yoshimura, M. Takano, M. Ceretti, C. Ritter, W. Paulus, *Nature* **450**, 1062-1065 (2007)
[8] Kageyama H., T. Watanabe, Y. Tsujimoto, A. Kitada, Y. Sumida, K. Kanamori, K. Yoshimura, N. Hayashi, S. Muranaka, M. Takano, M. Ceretti, W. Paulus, C. Ritter, G. André, *Angew. Chem. Int. Ed*. 47, 5740-5745 (2008)
[9] Gallagher P. K. J. B. MacChenney D. N. E. Buchanan, J Chem. Phys. 1966, 45, 246 –2471;
[10] LeToquin R., W. Paulus, A. Cousson, C. Prestipino, C. Lamberti J. Am. Chem. Soc. 2006, 128, 13161 – 13174
[11] Hayward M. A., M. J. Rosseinsky, Nature 2007, 450, 960 – 961

Contact :   **gilles.andre@cea.fr**